ORIGINAL ARTICLE

Cancer Science WILEY

Targeted exosome-encapsulated erastin induced ferroptosis in triple negative breast cancer cells

Mengyu Yu[1,2] | Chengcheng Gai[1,2] | Zihaoran Li[1] | Dejun Ding[3] | Jie Zheng[1] (iD) | Weifen Zhang[2,3] | Shijun Lv[1] | Wentong Li[1,2] (iD)

[1]Department of Pathology, Weifang Medical University, Weifang, China

[2]Collaborative Innovation Center for Target Drug Delivery System, Weifang Medical University, Weifang, China

[3]Department of Pharmacology, Weifang Medical University, Weifang, China

Correspondence
Shijun Lv and Wentong Li, Department of Pathology, Weifang Medical University, Weifang, Shandong Province 261053, China.
Email: sjlu@wfmc.edu.cn; liwentong11@163.com

Funding information
National Natural Science Foundation of China, Grant/Award Number: 81472365, 81774125 and 81802474

Abstract

Ferroptosis is an iron-dependent, lipid peroxide-driven cell death caused by inhibition of the cystine/glutamate transporter, which is of importance for the survival of triple-negative breast cancer (TNBC) cells. Erastin is a low molecular weight chemotherapy drug that induces ferroptosis; however, poor water solubility and renal toxicity have limited its application. Exosomes, as drug delivery vehicles with low immunogenicity, high biocompatibility and high efficiency, have attracted increasing attention in recent years. Herein, we developed a formulation of erastin-loaded exosomes labeled with folate (FA) to form FA-vectorized exosomes loaded with erastin (erastin@FA-exo) to target TNBC cells with overexpression of FA receptors. The characterization, drug release, internalization and anti–tumor effect in vitro of erastin@FA-exo were determined. Erastin@FA-exo could increase the uptake efficiency of erastin into MDA-MB-231 cells; compared with erastin@exo and free erastin, erastin@FA-exo has a better inhibitory effect on the proliferation and migration of MDA-MB-231 cells. Furthermore, erastin@FA-exo promoted ferroptosis with intracellular depletion of glutathione and reactive oxygen species overgeneration. Western blot analyses revealed that erastin@FA-exo suppressed expression of glutathione peroxidase 4 (GPX4) and upregulated expression of cysteine dioxygenase (CDO1). We conclude that targeting and biocompatibility of exosome-based erastin preparations provide an innovative and powerful delivery platform for anti–cancer therapy.

KEYWORDS

erastin, exosomes, ferroptosis, reactive oxygen species, triple negative breast cancer

1 | INTRODUCTION

Triple-negative breast cancer (TNBC) is a specific subtype of breast cancer with higher rates of distant recurrence and mortality than other types of breast cancer.[1] Because TNBC lacks the expression of progesterone receptor (PR), estrogen receptor (ER) and human epidermal growth factor receptor (HER2), current EGFR-targeted therapy and hormone therapy are ineffective in treating TNBC.[2] In addition, the availability of chemotherapy drugs for TNBC is very limited in the clinic. Thus, providing effective and targeted treatment of TNBC with anti–cancer drugs remains a challenge.[3,4]

Ferroptosis is a different type of cell death from the traditional apoptosis and necrosis, which is caused by the accumulation of

iron-dependent lipid peroxide.[5] Erastin is a low molecular chemo-therapeutics drug; some TNBC cells are reportedly sensitive to erastin-induced ferroptosis[6,7]; however, erastin is limited by its low water solubility and nephrotoxicity. Therefore, drug delivery systems with high efficiency and low side effects are needed to delivery erastin.

Over the past decade, nanotechnology and targeted drug delivery have received a lot of attention.[8] Unfortunately, application of nanotechnology-based chemotherapy is severely challenged for several reasons, including cytotoxicity, loss of targeting and rapid clearance by the reticuloendothelial system.[9,10] Recently, many new nano-carrier materials have emerged, and exosomes, as one of them, have attracted much attention. Exosomes, composed of lipid bilayer and rich in adhesive proteins, are micro membrane vesicles approximately 30-100 nm in diameter secreted by cells, which readily interact with cellular membranes and deliver drugs to cells.[11,12] Therefore, exosomes are being increasingly studied as drug delivery vectors.[13-15]

Recent studies have reported that exosomes could load low molecular chemotherapeutic drugs.[16,17] Therefore, we apply ultrasonic waves to load erastin into FA-labeled exosomes to develop an improved formulation targeting TNBC for systemic administration.[18] Our investigation revealed a robust accumulation of erastin and a more effective killing effect of systemically administered erastin@FA-exo in TNBC cells.

2 | MATERIALS AND METHODS

2.1 | Cells culture

MDA-MB-231 (human TNBC cell line) and HFL-1 (human fetal lung fibroblasts) were obtained from ATCC and were maintained at 37°C in a humidified 5% CO_2 atmosphere; MDA-MB-231 cells and HFL-1 cells were cultured using complete RPMI 1640 and Ham's F-12K medium (supplemented with 10% FBS, 1% penicillin and streptomycin) (Cyclone Utah, USA), respectively.

2.2 | Isolation and characterization of exosome from HFL-1 cells

To isolate exosomes, HFL-1 cells were cultured in serum-free medium for 48 hours and exosomes were isolated by differential centrifugation. In brief, cell debris and large vesicles were removed from the supernatant by centrifugation at 300 g for 10 minutes, 1000 g for 20 minutes and 10 000 g for 30 minutes. The samples were then rotated for 1 hour at a speed of 100 000 g, and exosomes were purified and collected. Protein concentration was determined using a BCA kit (Pierce Biotechnology), and exosomes were re-suspended in PBS (40 μg/mL, total protein). Exosomes were characterized by transmission electron microscopy (TEM, Philips) and dynamic light scattering (DLS, Zetasizer Nano system). Exosomes were lysed with RIPA lysis buffer (Sigma). The expression of exosomal proteins of TSG101 and CD81 was determined by western blot.

2.3 | The synthesis and optimization of erastin@FA-exo

Targeted exosomes labeled with DSPE-PEG$_{2000}$-FA (Shanghai Ponsure Biotechnology) was prepared as follows: 1 mL purified exosomes were mixed with DSPE-PEG$_{2000}$-FA at 37°C for 30 minutes. Erastin (1 mg, MedChemExpress) was added to the FA-exo (1 mL) and the mixture was sonicated (500 v, 2 kHz, 20% power, 6 cycles by 4 second pulse and 2 second pause), with a 2-minute cooling period between each cycle.[16] The solution was then incubated at 37°C for 1 hour to restore the exosomal membrane to form erastin@FA-exo. Excess free FA and erastin were eliminated from the solution by size exclusion chromatography.

To determine the most appropriate concentration of FA, different concentrations of DSPE-PEG$_{2000}$-FA (0-80 μg/mL) were added into exosomes (40 μg/mL, total protein), and then added to MDA-MB-231 cells to detect the internalization and obtain the optimal concentration.

2.4 | Loading capacity and in vitro release

The content of erastin in exosomes was determined by HPLC (Agilent 1200, Agilent Technologies). To evaporate solvent, erastin@FA-exo (100 μL) was heated at 70°C. Then, the same volume of acetonitrile was added, after ultrasound, centrifuging at 24 000 g for 10 minutes. The supernatant was filtered with a 2-μm syringe filter and 20-μL aliquots were transferred into HPLC autosampler vials. To measure erastin release, free erastin and freshly prepared erastin@FA-exo were loaded in a 300K MWCO device, respectively. Samples were taken at different time points and analyzed using HPLC, expressed as the percentage of erastin released divided by total erastin.

2.5 | Internalization of drug-loaded exosomes

To quantify the amount of erastin@FA-exo and erastin@exo taken up by MDA-MB-231 cells, lipophilic fluorescent dye PKH26 (MaoKang Biotechnology) was used to stain the exosomes. To detect the effect of FA receptor binding on cell uptake, culture medium containing 1.1 mg/mL of free FA was added to MDA-MB-231 cells to competitively inhibit FA receptors. After incubation for 6 hours, the cells were washed with PBS 3 times.[19] Then erastin@FA-exo was added and the cells' uptake of the drug was observed.

Subsequently, to quantify the amount of erastin@FA-exo and erastin@exo taken up by MDA-MB-231 cells, erastin@FA-exo $_{(PKH26)}$ and erastin@exo $_{(PKH26)}$ were added in equal amounts and incubated with MDA-MD-231 cells. Then the cells were washed with PBS at indicated times and fixed with 4% paraformaldehyde for 10 minutes; cells were stained with Hoechst at room temperature for 5 minutes. The cells were observed by fluorescence microscopy (Olympus X-73).

Meanwhile, we measured the uptake of erastin@FA-exo, erastin@exo and free erastin in MDA-MD-231 cells at 1 and 2 hours.

In brief, the cells were lysed with Triton x-100 and ultrasound was performed on ice. The lysed cell fluid was centrifuged at 67 000 g for 5 minutes, and the supernatant (20 μL) was determined by HPLC.

2.6 | Cell viability assay

MDA-MB-231 cells were seeded in a 96-well plate and treated with erastin@FA-exo, erastin@exo or free erastin at 37°C for 48 hours. Cytotoxicity of drugs was determined by MTT assay. Absorbance detection was performed with the iMark Microplate Reader (Bio-Rad) at the wavelength of 490 nm. Meanwhile, to verify the effect of FA-exo on cell growth, 0-40 μg/mL FA-exo was added to MDA-MB-231 cells, and cell viability was determined by MTT assay.

2.7 | Measurement of reactive oxygen species levels

MDA-MB-231 cells were seeded in a 6-well plate and treated with erastin@FA-exo, erastin@exo or free erastin. After 8 hours, 20 μM 2′, 7′-dichlorofluorescin diacetates (Beyotime Biotechnology) was used to stain the cells at 37°C for 30 minutes in the dark, and the intracellular reactive oxygen species (ROS) level was observed by fluorescence microscopy.

2.8 | Malondialdehyde assay

A malondialdehyde (MDA) detection kit (Solarbio) was used to determine the relative concentration of malondialdehyde in the cell lysate, according to the instructions of the manufacturer. The content of the MDA-TBA adduct formed by the reaction of MDA and thiobarbituric acid (TBA) was determined by colorimetric method.

2.9 | Glutathione content

Intracellular glutathione (GSH) content was determined using the Glutathione Assay Kit (Beyotime Biotechnology). GSH levels of MDA-MB-231 cells were detected after different treatments according to the instructions of the kit. GSH can react with DTNB to form a complex, which was determined at 412 nm, and the absorbance was proportional to the content of GSH.

2.10 | Western blot analysis

The treated cells were lysed and supernatant was collected. The protein concentration was detected using a BCA assay. Cell lysate was resolved by 10% SDS-PAGE gels and then transferred into nitrocellulose membrane. Blocking with 0.5% BSA in TBST for 1 hour followed. Membranes were incubated with primary antibodies overnight at 4°C, and then incubated with appropriate secondary antibodies at 37°C for 1 hour. The immunoreactive bands were revealed by enhanced chemiluminescence (Pierce).

2.11 | JC-1 mitoscreen assay

After treatment with erastin@FA-exo, erastin@exo or free erastin for 24 hours, the mitochondrial membrane potential of MDA-MB-231 cells was detected using the JC-1 Apoptosis Detection Kit (Biotechnology). This assay was performed according to the instructions of the kit, and, finally, the cells were imaged by fluorescence microscopy.

2.12 | Colony forming assay

Three hundred cells per well were seeded in a 6-well plate. After different treatments, the cells were further cultured for another 14 days. The cells were fixed with 4% paraformaldehyde and stained with 0.1% crystal violet.

2.13 | 5-ethynyl-2′-deoxyuridine assay

MDA-MB-231 cells were seeded in 24-well plates overnight. After different treatments, the cells were further cultured for another 24 hours, and the proliferation rate was detected using a 5-ethynyl-2′-deoxyuridine (EdU) Cell Proliferation Kit (Beyotime Biotechnology). The EdU was added to the cells and incubated for 2 hours at 37°C, stained with Hoechst for 5 minutes after being fixed with 4% paraformaldehyde. The cells were observed by fluorescence microscopy, and the EdU-positive percentage of the cells was calculated by taking 3 wells in each group.

2.14 | Wound healing assay

MDA-MB-231 cells (2.5×10^5) were seeded in 6-well plates, and 100% confluence was achieved. Cells were scratched in the center of the well with a 200-μL pipette tip. Cells were treated with erastin@FA-exo, erastin@exo or free erastin, respectively. Images were collected at 0, 24 and 48 hours under an inverted microscope. The wound area was measured by ImageJ.

2.15 | Flow cytometric analysis

For cell ferroptosis analysis, cells were seeded at a density of 2.5×10^5 cells per well in 6-well plates, and treated with erastin@FA-exo, erastin@exo or free erastin for 24 hours. The percentage of cells undergoing apoptosis was measured using flow cytometry with 7-ADD and Annexin-V double staining. Flow cytometry analysis was undertaken by counting 1×10^4 cells.

2.16 | Statistical analysis

SPSS 22.0 was used for data analysis, at least 3 times for each experiment, and mean ± SD was used for the results. The significance level was defined as $P < 0.05$, *$P < 0.05$, **$P < 0.01$, ***$P < 0.001$.

3 | RESULTS

3.1 | Preparation and characterization of erastin@FA-exo

The preparation process for erastin@FA-exo was as follows. In brief, exosomes were extracted from the culture medium of HFL-1 cells, modified with targeted FA, and, finally, erastin was loaded into FA-exo by ultrasound (Figure 1).

The average diameter of naive exosomes was 88.45 ± 19.53 nm, as shown by DLS analysis, (polydispersity index of 0.343; Figure 2a). The results of TME demonstrated that naive exosomes were uniform in size, and similar in size to those measured by DLS (Figure 2b). The morphology of exosomes was retained after drug loading by sonication (Figure 2d). DLS showed that the particle size of exosomes was 110.69 ± 21.78 nm, which was increased compared with naive exosomes (Figure 2c). In addition, western blotting showed more enriched TSG101 and CD81 exosomal markers in exosomes compared with cell lysate,[20,21] confirming that the isolated granules were exosomes (Figure 2e).

In subsequent uptake experiments, we determined that 40 μg DSPE-PEG$_{2000}$-FA/mg protein could maximize the uptake rate of MDA-MB-231 cells (Figure 2f). The FA content continued to increase, and the cell intake was not significantly increased, which was suitable for subsequent experiments.

The erastin loading was 3.2 mg erastin/mg protein. The in vitro release spectrum of erastin was determined in PBS (pH 7.4); erastin release of erastin@FA-exo reached 45% within the first 4 hours with sustained slow release spectrum later (Figure 2g).

3.2 | Cellular accumulation and cytotoxicity of erastin@FA-exo

Receptor targeting was assessed by FA-vectorized exosomes into FA receptor blocked MDA-MB-231 cells. Cell uptake assay demonstrated that the uptake rate of FA-exo in MDA-MB-231 cells with FA receptor blocked was significantly lower than that in MDA-MB-231 cells without free FA treatment (Figure 3a).

Endocytosis is a critical process in which exosomes transmit information to target cells.[22] Here, erastin@FA-exo and erastin@ exo labeled PKH26 were incubated with MDA-MB-231 cells; compared with erastin@exo, erastin@FA-exo was more internalized in MDA-MB-231 cells (Figure 3b). Meanwhile cell uptake assay demonstrated that erastin@FA-exo can more efficiently transport erastin into MDA-MB-231 cells than erastin@exo and free erastin (Figure 3c).

Moreover, we demonstrate that FA-exo at various concentrations has no influence on MDA-MB-231 cells (Figure 3d). To assess the efficacy of elastin-loaded exosomal preparations, MDA-MB-231 cells were treated with increasing concentrations of erastin (10-80 μM) and subjected to the MTT assay 48 hours later to assess cell viability. The results showed that erastin@FA-exo was significantly more effective in killing tumor cells than erastin@exo and free erastin (Figure 3e).

3.3 | Erastin@FA-exo suppressed MDA-MB-231 cell proliferation and migration

5-ethynyl-2′-deoxyuridine (EdU) and colony formation assays indicated that erastin@FA-exo could restrain cell proliferation significantly compared with free erastin or erastin@exo (Figure 4a,b). Following treatment with 10 μM of erastin@FA-exo for 24 and 48 hours, the erastin@FA-exo treated MDA-MB-231 cells showed a significant reduction of wound closure (Figure 4c).

3.4 | Erastin@FA-exo caused mitochondrial dysfunction and overgeneration of reactive oxygen species

Erastin has been reported to play a critical role in inducing ferroptosis via ROS accumulation.[6] In our study, DCFH-DA staining results showed that the ROS intensity of MDA-MB-231 cells treated with erastin@FA-exo was significantly increased (Figure 5a). Because MDA is one of the most important end products of lipid peroxidation, the MDA level in cells was also measured. Erastin@FA-exo increased the MDA level in MDA-MB-231 cells more obviously (Figure 5b), indicating that erastin@FA-exo are much more efficient than erastin@exo and free erastin.

Erastin consumes GSH by inhibiting the x_c^- system, which, in turn, triggers ferroptosis. Therefore, we measured GSH levels in
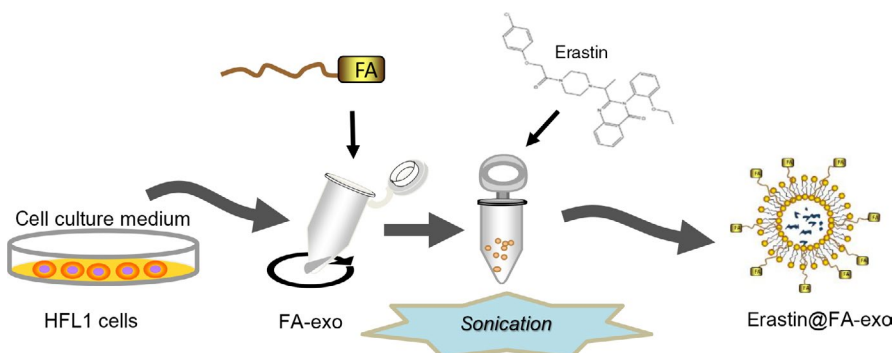

FIGURE 1 Diagram of preparation for erastin@FA-exo

FIGURE 2 Characterization of erastin@FA-exo. A, Size distribution of naive exosomes determined by dynamic light scattering (DLS). B, Representative transmission electron microscopy (TEM) image of naive exosomes derived from HFL-1 cells. C, Size distribution of erastin@FA-exo determined by DLS. D, TEM image of erastin@FA-exo. E, TSG101 and CD81 expressions of exosomes by western blot. F, The uptake of erastin@FA-exo with different DSPE-PEG$_{2000}$-FA contents was detected by fluorescence quantitative analysis. G, In vitro release of erastin from erastin@FA-exo in pH 7.4 by HPLC
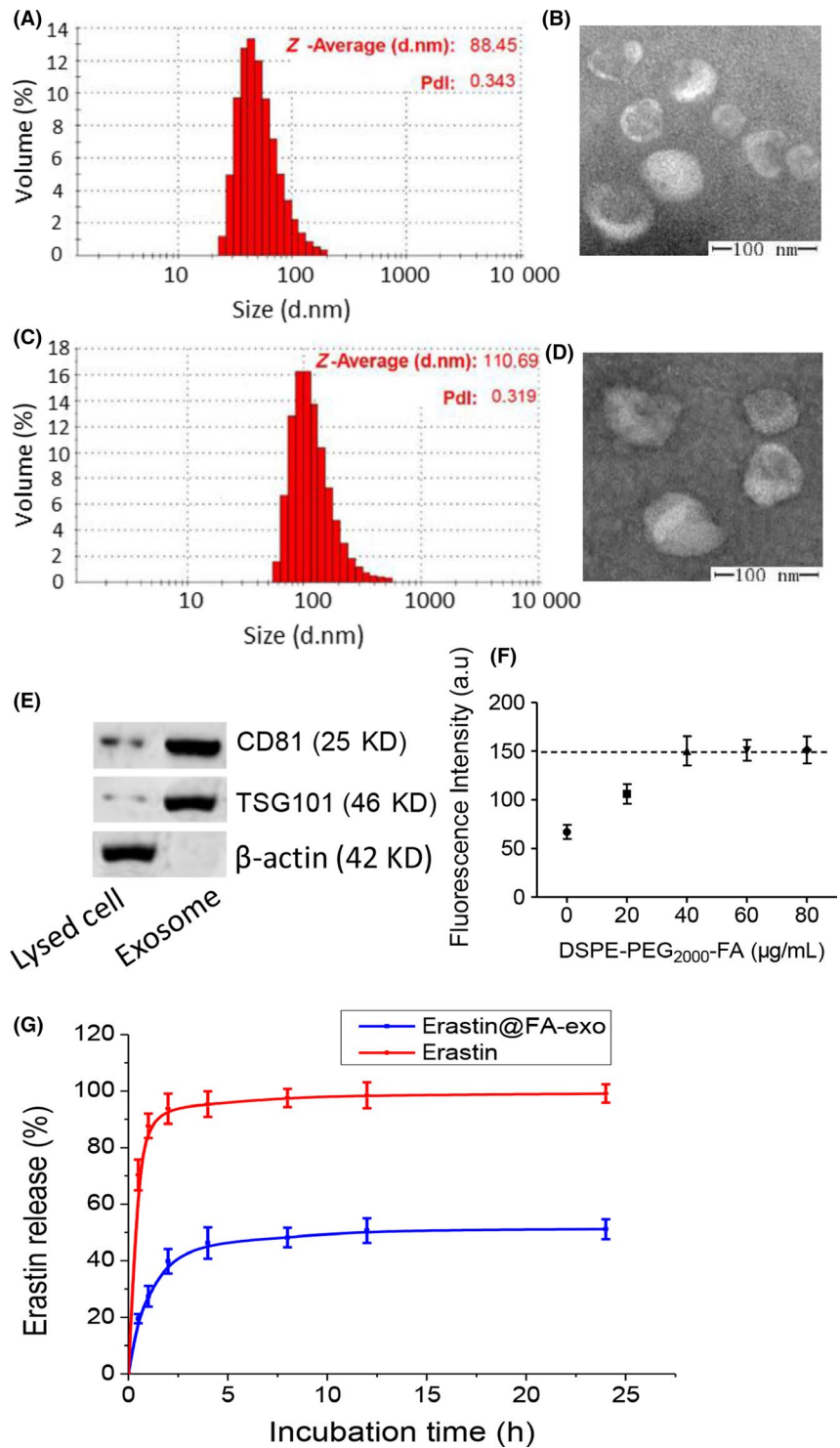
MDA-MB-231 cells, and the results showed that the GSH level in MDA-MB-231 cells treated with erastin@FA-exo was significantly lower than that in the other 2 treatment groups (Figure 5c). Next, we assessed mitochondrial dysfunction by evaluating mitochondrial membrane potential. Compared with the erastin@exo and the free erastin, erastin@FA-exo exhibited mitochondrial membrane potential change in MDA-MB-231 cells (Figure 5d).

3.5 | Erastin@FA-exo suppressed GPX4 and upregulated CDO1

We examined the glutathione peroxidase 4 (GPx4) and cysteine dioxygenase 1 (CDO1) by western blot after the different treatment. The expression of CDO1 in MDA-MB-231 cells treated with erastin@FA-exo was higher than that of erastin@exo and free erastin,
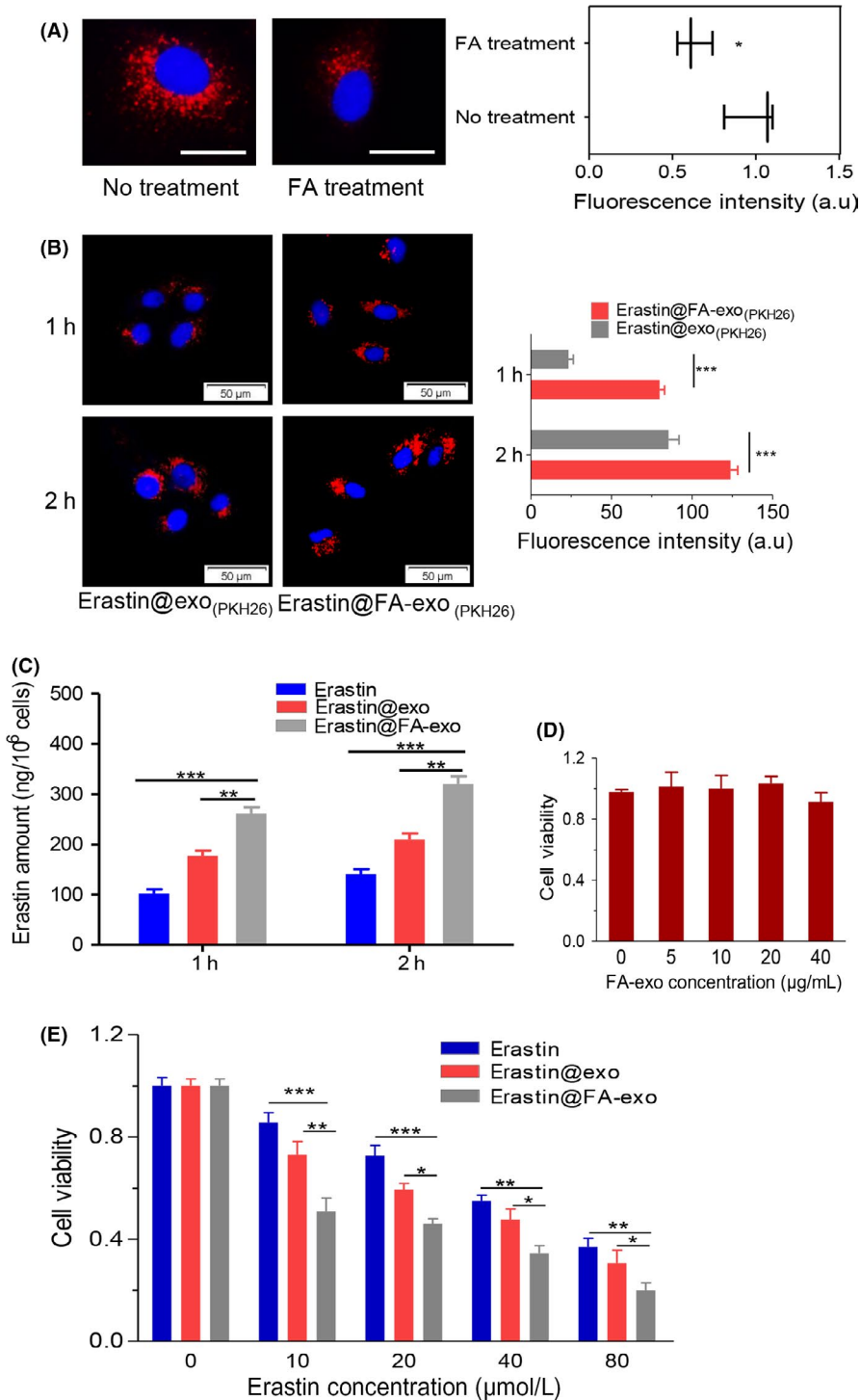
FIGURE 3 Cellular accumulation and cytotoxicity of erastin@FA-exo. A, MDA-MB-231 cells were treated with free folate (FA); internalization was measured by fluorescence quantitative analysis; bar = 20 μm. B, Exosome uptake was observed by fluorescence microscopy. C, Intracellular erastin concentration of MDA-MB-231 cells treated with free erastin, erastin@exo and erastin@FA-exo. D, Cell viability of MDA-MB-231 cells in response to treatment with FA-exo. E, Cell viability of MDA-MB-231 cells when pretreated with erastin@FA-exo, erastin@exo or free erastin treatments

and the expression of GPX4 was also significantly lower than that of the other 2 groups (Figure 6).

3.6 | Erastin@FA-exo induced ferroptosis effects on MDA-MB-231 cells

Flow cytometry was used to measure the ferroptosis of MDA-MB-231 cells; erastin@FA-exo induced ferroptosis was more obvious than that of other groups (Figure 7a), which was confirmed by morphologically dying cells (Figure 7b).

4 | DISCUSSION

The recognition that some tumors are highly sensitive to ferroptosis suggests that ferroptosis inducers have high therapeutic indices for cancer.[23,24] Erastin causes ROS-dependent cell ferroptosis by inhibiting system x_c^-, which is responsible for the translocation of intracellular glutamate to the extracellular space and extracellular cystine to the cell.[5,6] TNCB is auxotrophic for glutamine and relies on the deamination of glutamine by glutaminase to glutamate to fuel xCT, which underscores the importance of this pathway in the survival of
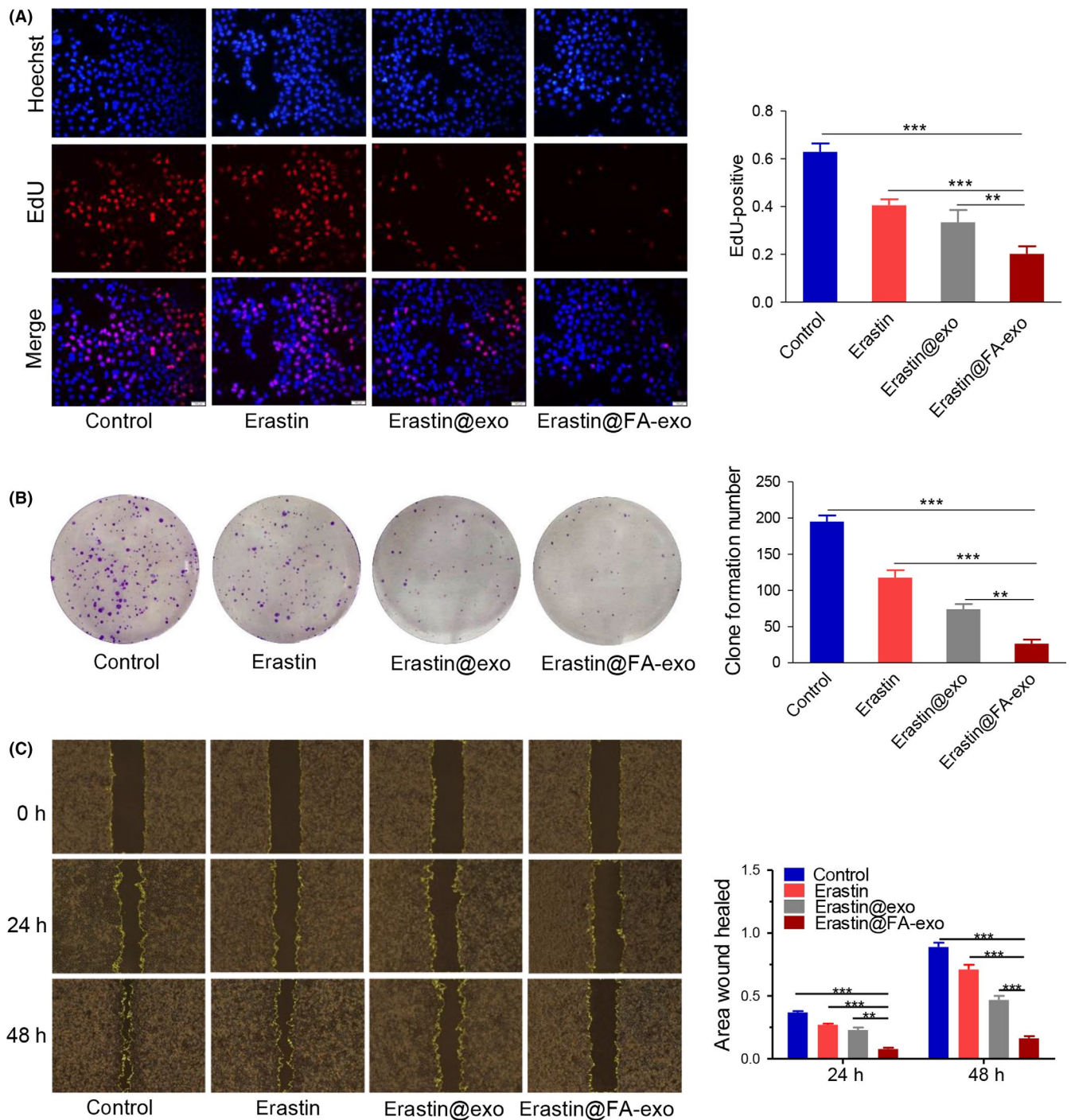
FIGURE 4 Erastin@FA-exo suppressed MDA-MB-231 cell proliferation and migration. A, The effects of erastin@FA-exo, erastin@exo and free erastin on proliferation of MDA-MB-231 cells were performed by 5-ethynyl-2′-deoxyuridine (EdU). B, Numbers of clone formation of MDA-MB-231 cells after different treatments. C, The effects of erastin@FA-exo, erastin@exo or free erastin on migration of MDA-MB-231 cells

TNBC cells.[7,25] Therefore, erastin was selected as the novel drug for TNBC in our experiment.

However, poor water solubility of erastin results in low absorption and limited bioavailability.[26] Therefore, an effective drug delivery method is needed to overcome these obstacles of chemotherapy based on erastin. Biomimetic nanomaterials have been extensively studied as drug delivery vectors, such as exosomes.[14] Exosomes are

a type of micro vesicle secreted by cells, which can transfer internal substances to surrounding cells efficiently through rich adhesion proteins interacting with cell membrane.[27,28] Based on the above, we selected HFL-1 cells as the maternal cells for the source of exosomes, which were characterized by DLS and TEM; the results showed that the average particle size was 88.45 ± 19.53 nm, with uniform size and typical vesicular structure. The particle size of exosomes increased
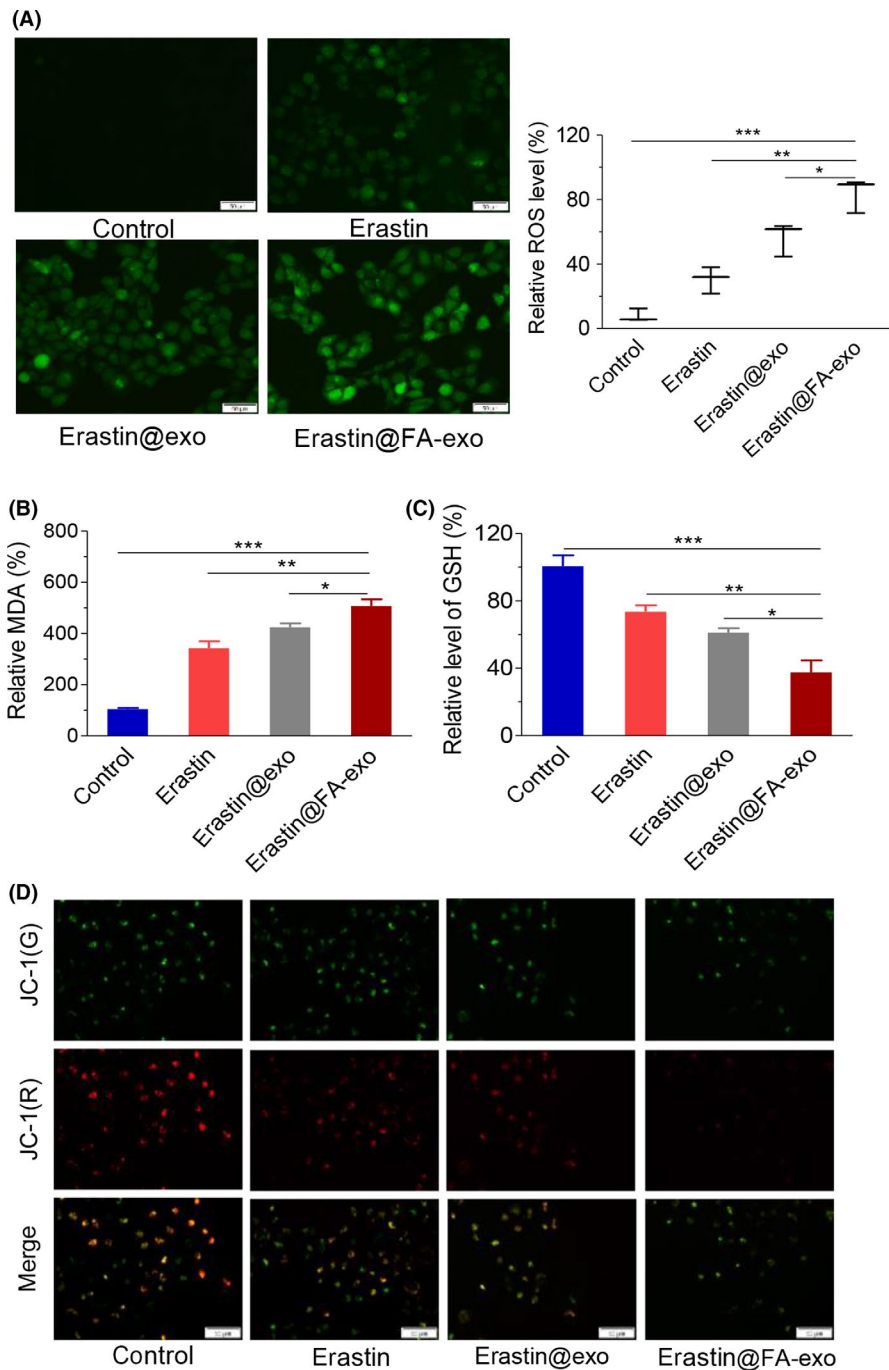
(A)

after ultrasonic loading, but the TEM showed that exosomes were still intact vesicles. In addition, the TSG10 and CD81 were characteristic of proteins of exosomes[21,29]; our results showed that TSG10 and CD81 were significantly enriched in exosomes.

Folate receptor was reported to be overexpressed in TNBC cells.[18] Thus, FA, a specific ligand for FA receptor, was selected to increase the selectivity of exosomes to TNBC cells. We optimized the amount of FA-modified exosomes and loaded erastin into vectorized exosomes. Because erastin is a highly hydrophobic compound, to prevent erastin from being integrated into the internal region of the relatively dense lipid bilayer in exosomes, sonication was performed to reshuffle the lipid bilayer to load erastin into

exosomes while maintaining the structural integrity of their membranes.[10,16] Results of in vitro release indicated that erastin@FA-exo reached the release amount of 47% within the first 4 hours, and the release trend gradually leveled off. Remarkably, half of the erastin was still present in the erastin@FA-exo at 24 hours, which means that erastin can be more efficiently transported to the tumor sites. In addition, nanometer drug delivery systems could interact with and internalize in target malignant tumor cells through FA-mediated tumor targeting.[30,31] Here, exosomes were labeled with FA for targeted drug delivery. The constructed erastin@FA-exo was preferentially ingested; thereby erastin was rapidly and massively accumulated in TNBC cells. FA-exo showed
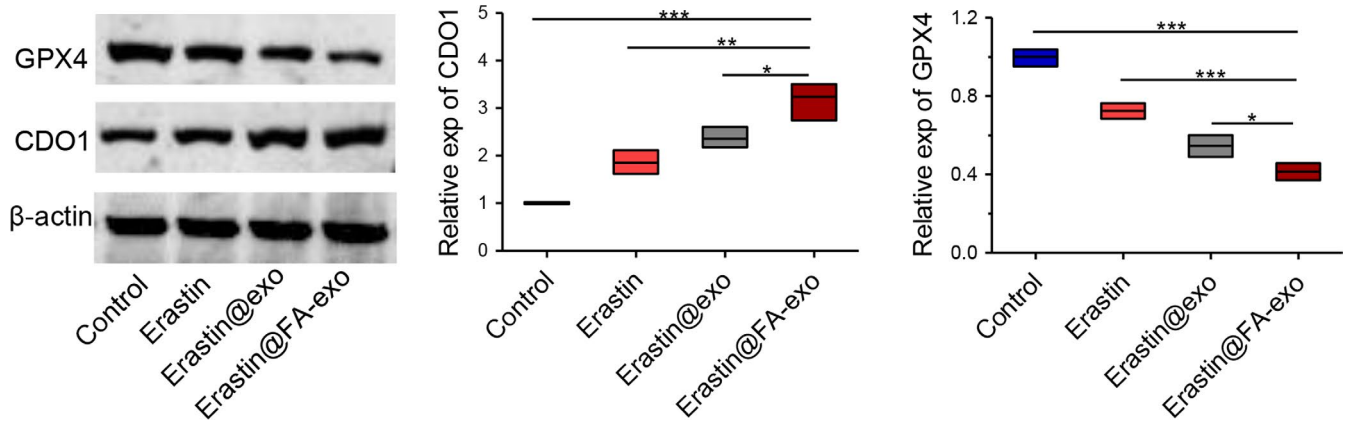
FIGURE 6 The expression levels of CDO1 and GPX4 proteins in MDA-MB-231 cells
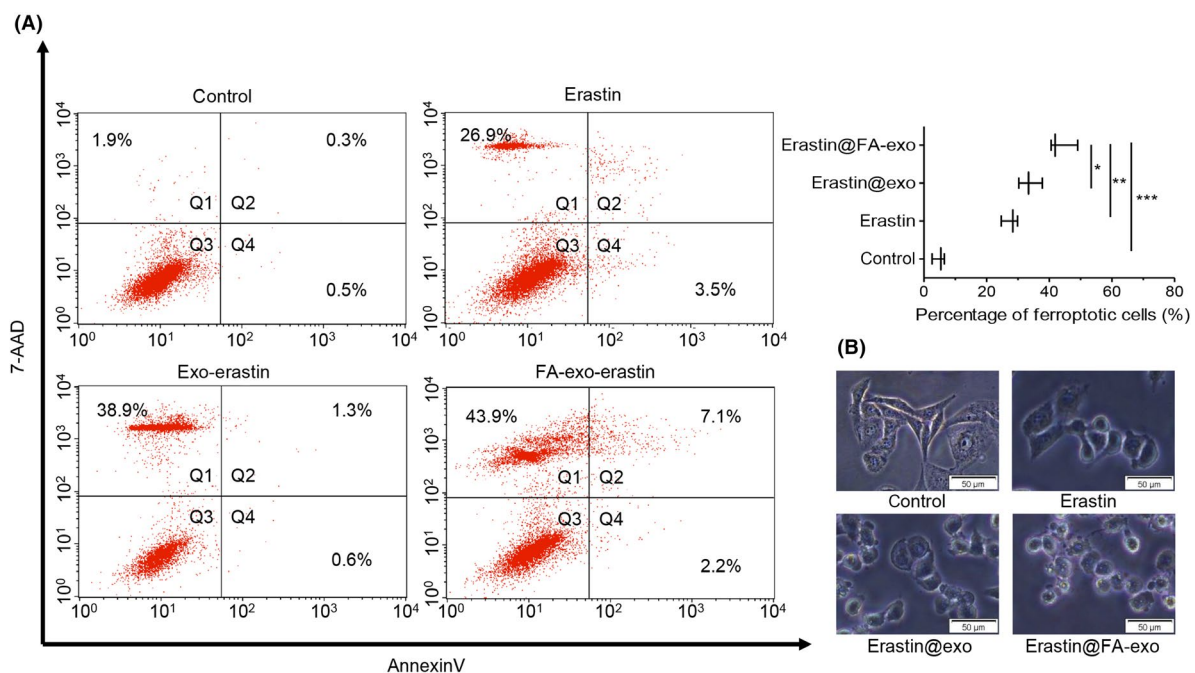

FIGURE 7 Erastin@FA-exo induced ferroptosis effects on MDA-MB-231 cells. A, Ferroptosis of MDA-MB-231 cell detected by flow cytometry. B, Morphologic changes of MDA-MB-231 cells

good cell compatibility, which could improve the efficiency of tumor treatment and avoid damage to healthy tissues. In addition, because erastin@FA-exo is more effective in delivering erastin to tumor cells, the inhibition rate of erastin@FA-exo on the cytotoxicity, proliferation and migration of MDA-MB-231 cells was much higher than that of erastin@exo and free erastin. We also found that erastin@FA-exo significantly increased ROS production and GSH consumption in MDA-MB-231 cells, and flow cytometry showed that erastin@FA-exo caused significantly more ferroptosis in MDA-MB-231 cells than erastin@exo and free erastin.

The erastin consumes GSH by inhibiting the system x_c^- that provides cystine for GSH synthesis, and GSH depletion can indirectly impair GPX4 function.[32] In the present study, we tested GPX4 in different treatment groups, and the GPX4 expression in the erastin@ FA-exo group was lower than erastin@exo or free erastin. In addition, GPX4 expression was dramatically decreased, while CDO1 was significantly upregulated, under erastin treatment.[33] The experiment results show that erastin@FA-exo was more effective in inhibiting GPX4 and upregulating CDO1 than erastin@exo and free erastin. Meanwhile we observed that erastin@FA-exo obviously reduced the mitochondrial membrane potential of MDA-MB-231 cells, inhibited the Warburg phenomenon of tumors, and promoted the generation of oxygen free radicals in tumor cells.

In brief, we proved that erastin@FA-exo can actively and selectively target MDA-MB-231 cells and efficiently induce ferroptosis in tumor cells. The exosome-targeted delivery system loaded with erastin might be a powerful platform for chemotherapy targeting TNBC.

DISCLOSURE

ORCID

Jie Zheng https://orcid.org/0000-0003-1526-0617

Wentong Li https://orcid.org/0000-0002-8855-2162

REFERENCES

1. Duncan J, Whittle M, Nakamura K, et al. Dynamic reprogramming of the kinome in response to targeted MEK inhibition in triple-negative breast cancer. *Cell*. 2012;149:307-321.
2. Kalimutho M, Parsons K, Mittal D, Lopez JA, Srihari S, Khanna KK. Targeted therapies for triple-negative breast cancer: combating a stubborn disease. *Trends Pharmacol Sci*. 2015;36:822-846.
3. Shah SP, Roth A, Goya R, et al. The clonal and mutational evolution spectrum of primary triple-negative breast cancers. *Nature*. 2012;486:395-399.
4. Lehmann BD, Bauer JA, Chen X, et al. Identification of human triple-negative breast cancer subtypes and preclinical models for selection of targeted therapies. *J Clin Invest*. 2011;121:2750-2767.
5. Yu H, Guo P, Xie X, Wang Y, Chen G. Ferroptosis, a new form of cell death, and its relationships with tumourous diseases. *J Cell Mol Med*. 2017;21:648-657.
6. Dixon SJ, Lemberg KM, Lamprecht MR, et al. Ferroptosis: an iron-dependent form of nonapoptotic cell death. *Cell*. 2012;149:1060-1072.
7. Timmerman LA, Holton T, Yuneva M, et al. Glutamine sensitivity analysis identifies the xCT antiporter as a common triple-negative breast tumor therapeutic target. *Cancer Cell*. 2013;24:450-465.
8. Peng Q, Zhang S, Yang Q, et al. Preformed albumin corona, a protective coating for nanoparticles based drug delivery system. *Biomaterials*. 2013;34:8521-8530.
9. Zou Y, Liu Y, Yang Z, et al. Effective and targeted human orthotopic glioblastoma xenograft therapy via a multifunctional biomimetic nanomedicine. *Adv Mater*. 2018;30:e1803717.
10. Haney MJ, Klyachko NL, Zhao Y, et al. Exosomes as drug delivery vehicles for Parkinson's disease therapy. *J Control Release*. 2015;207:18-30.
11. Cocucci E, Meldolesi J. Ectosomes and exosomes: shedding the confusion between extracellular vesicles. *Trends Cell Biol*. 2015;25:364-372.
12. Yu DD, Wu Y, Shen HY, et al. Exosomes in development, metastasis and drug resistance of breast cancer. *Cancer Sci*. 2015;106:959-964.
13. Kalani A, Kamat PK, Chaturvedi P, Tyagi SC, Tyagi N. Curcumin-primed exosomes mitigate endothelial cell dysfunction during hyperhomocysteinemia. *Life Sci*. 2014;107:1-7.
14. Tian Y, Li S, Song J, et al. A doxorubicin delivery platform using engineered natural membrane vesicle exosomes for targeted tumor therapy. *Biomaterials*. 2014;35:2383-2390.
15. Kanchanapally R, Deshmukh SK, Chavva SR, et al. Drug-loaded exosomal preparations from different cell types exhibit distinctive loading capability, yield, and antitumor efficacies: a comparative analysis. *Int J Nanomed*. 2019;14:531-541.
16. Kim MS, Haney MJ, Zhao Y, et al. Engineering macrophage-derived exosomes for targeted paclitaxel delivery to pulmonary metastases: in vitro and in vivo evaluations. *Nanomedicine*. 2018;14:195-204.
17. Kim MS, Haney MJ, Zhao Y, et al. Development of exosome-encapsulated paclitaxel to overcome MDR in cancer cells. *Nanomedicine*. 2016;12:655-664.
18. You C, Wang M, Wu H, et al. Near infrared radiated stimulus-responsive liposomes based on photothermal conversion as drug carriers for co-delivery of CJM126 and cisplatin. *Mater Sci Eng C Mater Biol Appl*. 2017;80:362-370.
19. Li H, Miteva M, Kirkbride KC, et al. Dual MMP7-proximity-activated and folate receptor-targeted nanoparticles for siRNA delivery. *Biomacromol*. 2015;16:192-201.
20. Lin LY, Du LM, Cao K, et al. Tumour cell-derived exosomes endow mesenchymal stromal cells with tumour-promotion capabilities. *Oncogene*. 2016;35:6038-6042.
21. Sun D, Zhuang X, Xiang X, et al. A novel nanoparticle drug delivery system: the anti-inflammatory activity of curcumin is enhanced when encapsulated in exosomes. *Mol Ther*. 2010;18:1606-1614.
22. Luga V, Zhang L, Viloria-Petit AM, et al. Exosomes mediate stromal mobilization of autocrine Wnt-PCP signaling in breast cancer cell migration. *Cell*. 2012;151:1542-1556.
23. Nagano O, Okazaki S, Saya H. Redox regulation in stem-like cancer cells by CD44 variant isoforms. *Oncogene*. 2013;32:5191-5198.
24. Chen RS, Song YM, Zhou ZY, et al. Disruption of xCT inhibits cancer cell metastasis via the caveolin-1/β-catenin pathway. *Oncogene*. 2009;28:599-609.
25. Conrad M, Angeli JP, Vandenabeele P, Stockwell BR. Regulated necrosis: disease relevance and therapeutic opportunities. *Nat Rev Drug Discov*. 2016;15:348-366.
26. Yu Y, Xie Y, Cao L, et al. The ferroptosis inducer erastin enhances sensitivity of acute myeloid leukemia cells to chemotherapeutic agents. *Mol Cell Oncol*. 2015;2:e1054549.
27. Antimisiaris SG, Mourtas S, Marazioti A. Exosomes and exosome-inspired vesicles for targeted drug delivery. *Pharmaceutics*. 2018;10.
28. Wang J, Zheng Y, Zhao M. Exosome-based cancer therapy: implication for targeting cancer stem cells. *Front Pharmacol*. 2016;7:533.
29. Wan Y, Wang L, Zhu C, et al. Aptamer-conjugated extracellular nanovesicles for targeted drug delivery. *Can Res*. 2018;78:798-808.
30. Lineton W, Azevedo M. Thermal oxidation protective surface for steel pistons. *Biomaterials*. 2016;76:115-132.
31. Feng B, Xu Z, Zhou F, et al. Near infrared light-actuated gold nanorods with cisplatin-polypeptide wrapping for targeted therapy of triple negative breast cancer. *Nanoscale*. 2015;7:14854-14864.
32. Dächert J, Schoeneberger H, Rohde K, Fulda S. RSL3 and erastin differentially regulate redox signaling to promote Smac mimetic-induced cell death. *Oncotarget*. 2016;7:63779-63792.
33. Hao S, Yu J, He W, et al. Cysteine dioxygenase 1 mediates erastin-induced ferroptosis in human gastric cancer cells. *Neoplasia*. 2017;19:1022-1032.